International Journal of Environmental Science and Technology (2022) 19:11857–11866
https://doi.org/10.1007/s13762-022-03989-0

ORIGINAL PAPER

Influence of pyrolysis temperature and feedstock biomass on Cu^{2+}, Pb^{2+}, and Zn^{2+} sorption capacity of biochar

M. A. Geleto[1] · R. Forján[2] · E. Arco-Lázaro[1] · E. F. Covelo[1] · P. Marcet[1] · B. Cerqueira[1,3]

Received: 4 November 2020 / Revised: 28 November 2021 / Accepted: 17 January 2022 / Published online: 21 February 2022
© The Author(s) 2022

Abstract

Biochar has attracted significantly growing attention due to its effectiveness in terms of both cost and environmental safety in removing trace metals from soil and water. Its metal sorption capacity depends on its properties, which are in turn governed by pyrolysis temperature and type of biomass. Therefore, this study examines the role of pyrolysis temperature and biomass in biochars sorption capacity of Pb^{2+}, Cu^{2+} and Zn^{2+}. Biochars produced by pyrolysis of maize (*Zea mays L.*) cobs at different temperatures were used to assess the effect of temperature, whereas evergreen oak (*Quercus ilex* L.) pyrolyzed at 500 °C was used to assess the effect of biomass. Sorption isotherms were constructed by batch method and compared with Langmuir and Freundlich models. Most of the sorption isotherms displayed irregular curves and not all of the isotherms fitted the models. Therefore, sorption distribution coefficients and metal removal percentages were used to determine sorption capacities biochars for studied metals. Accordingly, *Quercus ilex* L. was most effective in sorbing all studied metals, which indicates the role of biomass. The maize biochar pyrolyzed at 500 °C was most effective among maize cob biochars, which revealed the influence pyrolysis temperature. The concentrations of added sorption solutions also played significant role in sorption, and consequently biochar pyrolyzed 350 °C was least effective. The targeted metals also affected the sorption as they compete for sorption sites. Thus, their selective sequence was in the order of $Pb^{2+} > Cu^{2+} > Zn^{2+}$.

Keywords Biochar · Sorption · Distribution coefficient · Trace metals · Selectivity sequences

Introduction

Soil pollution by metals is a global concern because of their persistence and toxic nature even in their low concentrations, and they are not biodegradable unlike organic pollutants. The problem is exacerbated because of rapid industrialization (Ayangbenro and Babalola 2017; Barakat 2011; Cetin 2016) and application of agrochemicals (Qu et al. 2016). Trace metals such as copper, lead, and zinc are among the metals found in soils and known to pose human health and environmental threats (Kumar et al. 2014; Swartjes 2011; Tóth et al. 2016).

The use biochar as sorbent is one of the most effective methods employed to remove metals from contaminated soil and water (Ahmad et al. 2016; Beesley and Marmiroli 2011; Puga et al. 2015; Qian et al. 2015). Biochar (B) is a carbonaceous product obtained by pyrolysis of feedstock under limited oxygen (Ahmad et al. 2012; Inyang et al. 2016). The feedstock can be sourced from wide range of plants, animals and industrial wastes (Elzobair et al. 2016; Inyang et al. 2016; Rosales et al. 2015). As a result, biochar has attracted substantial attention for its role in removing metals from soil and water, increasing crop yield as it increases soil fertility by retaining nutrients, co-composting and carbon sink over the years (Forján et al. 2016; Rodríguez-Vila et al. 2018; Sanchez-Monedero et al. 2018; Zhou et al. 2018).

Metal sorption process by biochar involves varies mechanisms. These mechanisms include electrostatic interaction between the binding sites on the surface of biochar, cation

Editorial responsibility: Samareh Mirkia.

✉ M. A. Geleto
gmatiamano@uvigo.es

[1] Faculty of Biology, Department of Plant Biology and Soil Science, University of Vigo, As Lagoas-Marcosende, 36310 Vigo, Pontevedra, Spain

[2] INDUROT and Environmental Technology, Biotechnology and Geochemistry Group, Universidad de Oviedo, Campus de Mieres, Mieres, Asturias, Spain

[3] The James Hutton Institute, Craigiebuckler, Aberdeen AB15 8QH, UK

exchange between elemental components in biochar and metals, metal complexation with functional groups of biochar, crystallization as a result of metal precipitation and reduced metal ions that can be sorbed onto the sorption sites (Ahmad et al. 2014; Dong et al. 2011; Inyang et al. 2016; Tan et al. 2015).

The physicochemical properties of biochar determine its sorption capacity. These properties include high pH, electrical conductivity (EC), cation exchange capacity (CEC), the elemental composition, surface charge, and functional groups (Klasson 2017; Li et al. 2017; Tan et al. 2015).

Zhao et al. (2020) reported physicochemical properties of biochar highly depend on feedstock types and their pyrolysis temperature. Additionally, the pyrolysis conditions such as heating rate, holding time and preparation of biomass for biochar production play great roles both in quantity and in quality of produced biochar (Kloss et al. 2012; Sohi et al. 2009Steiner 2016). The increase in pyrolysis temperature enhances properties of biochar such as surface area, porosity, stability, pH, organic matter, and electrical conductivity (Forján et al. 2016; Kupryianchyk et al. 2016). Different studies (Chen et al. 2011; Kupryianchyk et al. 2016; Melo et al. 2013) have demonstrated the increase of biochar metal sorption capacity with the increase of these properties. However, there are certain cases where the contrary was demonstrated. Uchimiya et al. (2012) reported that lead sorption was greater at 350 °C compared to 650 °C for biochar produced from poultry litter. This confirms that the sorption mechanisms depend on feedstock material, pyrolysis temperature, pyrolysis condition, and targeted metal among other factors.

Therefore, the objective of this study is to determine Cu^{2+}, Pb^{2+} and Zn^{2+} sorption capacity of maize (*Zea mays* L.*)* cob biochars (MB) pyrolyzed at different temperatures and biochar produced from different biomass feedstock evergreen oak (*Quercus ilex* L.*)* biochar (QB) in mixed metal solutions of different concentrations. This allows us to analyze the role of pyrolysis temperature in the case of maize cob biochars and the feedstock biomass by comparing biochars sourced from different biomass and pyrolyzed at the same temperature.

Materials and methods

Material

Shelled maize cobs collected from Galicia, northwest of Spain were air-dried in the storage of Centro De Valorización Ambiental Del Norte SL. Touro, A Coruña, Spain. The maize cobs were pyrolyzed under selected conditions. The Horbesal furnace was preheated at 105 °C with a heating rate of 20 °C/min. In each pyrolysis, round 2000 g of maize cob was charred at three different temperatures 350 °C, 500 °C, and 650 °C with the same heating rate under limited oxygen presence. The residence time for each biochar was 105, 74, and 38 min for 350 °C, 500 °C, and 650 °C pyrolysis temperatures, respectively. These biochars are designated as MB350, MB500 and MB650 with numbers corresponding to pyrolysis temperature. As the pyrolysis temperature increased, the amount of biochars produced from the biomass decreased which indicates the inverse relationships between the amount of biochar produced and pyrolysis temperatures. Consequently, 20.6% of biomass was lost for MB350, whereas 33.44% and 44.1% were lost for MB500 and MB650, respectively. The *Quercus ilex* L. biochar was purchased from Piroeco Bioenergy, S.L., Málaga, Spain and designated as QB500. Many studies have reported higher pyrolysis temperature results in higher sorption capacities (Hotová and Slovák 2015). On the other hand, Intani et al. (2018) recommended optimal pyrolysis at 588.42 °C for maize cob biochar. The novelty of this work is to determine the sorption capacity of biochars produced both below and above the stated ideal pyrolysis temperature.

Methods

Moisture content (MC) was determined by oven drying the biochars at 110 °C to constant weight. Biochars pH was determined with a pH meter electrode in 1:2.5 biochar/water extracts (Li and Xu 2015). The cation exchange capacity (CEC) was calculated by summation of cations (Ca^{2+}, Mg^{2+}, K^{+}, Na^{+}) extracted by 0.1 M $BaCl_2$ following Hendershot and Duquette method (1986) and analyzed by Inductively Coupled Plasma Optical Emission Spectrometry (ICP-OES) in a Perkin Elmer Optima 4300 DV device. Pseudototal metal concentrations of each biochar were obtained from extracts of 3:1 HCl/HNO_3 aqua regia acid digestion in a microwave oven (Milestone ETHOS 1) and the extracts were analyzed by an ICP-OES (Forján et al. 2016).

Batch sorption experiment

Batch sorption experiment was conducted according to the methods employed by Alberti et al. (1997) and Gomes et al. (2001), as modified by Harter and Naidu (2001). Biochar samples (1.5 g) were shaken with 25 ml metal solution prepared using mix of Cu^{2+}, Pb^{2+}, and Zn^{2+} nitrates (0.1, 0.5, 1, 2, and 3 mmol L^{-1}) with electrolyte background of 0.01 M $NaNO_3$ in polyethylene tubes on a plane shaker for 24 h at room temperature (Vega et al. 2008). The samples were then centrifuged 10 min at 3000 rpm and the supernatants were filtered through millex syringe filter (pore size 0.45 µm). To determine the concentrations of studied metals in each solution, the filtrates were analyzed by ICP-OES. The concentrations of each metal (Qe) that had been sorbed onto each biochar were determined by subtracting concentrations of equilibrium solutions (after shaking with biochar) from blank solutions (without biochar) (Eq. 1).

$$Q_e = \frac{(C_i - C_e)V}{w} \quad (1)$$

where C_i and C_e are the initial and equilibrium metal concentration (mg/L), w is the weight of dry biochar (g) and V is the volume of the added solution (mL).

The sorption isotherms were constructed for each metal by plotting the concentration of sorbed metal (μmolg^{-1} of dry biochar) against the concentration of the metal in solution at equilibrium (μmol L^{-1}).

The sorption isotherm parameters were obtained from Langmuir (2) and Freundlich models (3).

$$\text{Langmuir model:}\frac{x}{m} = \mathrm{CK_L}\beta_\mathrm{L}\left(1 + \mathrm{CK_L}\right) \tag{2}$$

x: quantity of sorbed metal (μmol). m: quantity of sorbent (g). C: Solution concentration at equilibrium (μmol L^{-1}). K_L: Langmuir constant (L μmol L^{-1}). β_L: high sorption capacity (μmol g^{-1}).

Freundlich model:

$$\mathrm{Log}\frac{x}{m} = 1/n\log C + \log K_\mathrm{F} \tag{3}$$

x: quantity of sorbed metal (μmol). m: quantity of sorbent (g). C: Solution concentration equilibrium (μmol L^{-1}). K_F: Freundlich constant (Lg^{-1}). n: dimensionless. $n > 1$, sorption favorable.

The sorption distribution coefficients (K_d) for the metals in each biochar at equilibrium were calculated from the ratio of concentration of metal sorbed (μmol g^{-1}) and concentration of metal in solution (μmol L^{-1}).

$$\text{Distribution coefficients } (K\mathrm{d}) = \frac{\text{Concent ration of metal sorbed}}{\text{Concentration of metal in solution}} \tag{4}$$

The combined distribution coefficients were calculated for each biochar according to the procedure by Kaplan et al. (1995) and Covelo et al. (2007) to determine the overall sorption capacity of biochar.

$$\mathrm{Kd}\Sigma\mathrm{sp} = \frac{\text{CMx biochar}}{\text{CMx solution)}} \tag{5}$$

where CMx, biochar and CMx, solution are the concentrations of metal x in the biochar (μmol g^{-1}) and its solution (μmol L^{-1}), respectively.

Finally, the percentage of metal removal (%MR) was calculated according to Desta (2013) using Eq. (6).

$$\%\mathrm{MR} = \frac{(Ci - Ce)}{\mathrm{Ci}} * 100\% \tag{6}$$

where C_i and C_e are the initial and equilibrium metal concentration (mg/L), respectively.

K_d values were used for estimation of the overall sorption capacity and the percentages of metals removal (%MR) were used to demonstrate the actual percentage of metals removed by the dosage of biochar (1.5 g) used in this study from added metal solution.

Statistical analyses

All the analytical tests were performed in triplicate, and the obtained data were statistically analyzed using SPSS version 24.0 for windows. Analysis of variance (ANOVA) and test of homogeneity of variance were carried out. In case of homogeneity, a Post Hoc least significant difference (LSD) test was carried out. If there was no homogeneity, Dunnett's T3 test was performed. Significant differences among biochars based on pyrolysis temperatures were determined using one-way analysis of variance (ANOVA). Independent t-test was performed to compare the roles of biomass between MB500 and QB500.The relationship among biochar parameters were determined by Pearson correlation analysis.

Results and discussion

Biochar characterization

The physicochemical characteristics of maize biochars used in this study are presented in Table 1. These properties varied based on the pyrolysis temperatures.

The pyrolysis temperature significantly influenced physicochemical characteristics of biochars ($p < 0.05$). The pH increased with increasing pyrolysis temperature (Table 1). This agrees the results obtained by Novak et al. (2009); Rafiq et al. (2016); Liu et al. (2014) and Wang et al. (2015a).

However, the pH values were not significantly different for MB500 and MB650, whereas they are significantly different from MB350 at $p < 0.05$ (see Table 1). The pH plays vital role when biochar is used to remove metals from aqueous solution. Solution pH highly affects the surface charge of biochar. When solution pH is greater than the point zero charge (pH_{pzc}) of biochar, i.e., solution pH at which its surface net charge is zero, biochar is negatively charged and vice versa. A negatively charged surface of biochar binds with cations and contributes to metal sorption. It also affects complexation of functional groups, which is one of metal sorption mechanisms by biochar (Li et al. 2017).

Carbon content also increased with the pyrolysis temperature and they were significantly different from each other at ($p < 0.05$). Similarly, pyrolysis temperature significantly increased EC Table 1. The CEC of MBC first increased and then decreased with increasing pyrolysis temperature. As shown in Table 1, CEC of MBC is significantly different from each other at $p < 0.05$.

The pyrolysis temperature also influenced the exchangeable cations concentration (Ca^{2+}, K^+, Mg^{2+}, and Na^+) showed varying results. Accordingly, Ca^{2+} and Mg^{2+} decreased with

Table 1 Physicochemical characterization of biochars based on pyrolysis temperature

Parameters		MB350	MB500	MB650
Biochar				
pH		8.87 ± 0.03b	10.26 ± 0.04a	10.29 ± 0.07a
EC	mS/cm	1.31 ± 0.29c	2.23 ± 0.23b	2.98 ± 0.16a
C	%	60.19 ± 0.18c	64.55 ± 0.37b	74.32 ± 0.55a
N		0.54 ± 0.01a	0.34 ± 0.04b	0.45 ± 0.08a
C/N		111.49 ± 1.97b	193.81 ± 25.20a	168.29 ± 26.65a
Pseudo total				
Cu^{2+}	(mg kg^{-1})	7.68 ± 0.56c	10.44 ± 0.39b	13.14 ± 1.75a
Pb^{2+}		u.l	u.l	u.l
Zn^{2+}		75.17 ± 23.20a	131.10 ± 27.48a	119.84 ± 7.70a
Extractable				
Cu^{2+}	(mg kg^{-1})	u.l	u.l	u.l
Pb^{2+}		u.l	u.l	u.l
Zn^{2+}		0.51 ± 0.03c	1.28 ± 0.17b	1.55 ± 0.17a
CEC	(cmol $_{(\pm)}$ kg^{-1})	15.23 ± 1.98c	50.54 ± 4.73a	31.99 ± 3.49b
Ca^{2+}		0.30 ± 0.07a	0.17 ± 0.02b	0.11 ± 0.01b
K^{+}		14.00 ± 1.70c	49.50 ± 4.65a	31.21 ± 3.41b
Mg^{2+}		0.68 ± 0.18a	0.29 ± 0.02b	0.23 ± 0.03b
Na^{+}		0.25 ± 0.03b	0.58 ± 0.05a	0.44 ± 0.04a

For each row, different letters in different samples mean significant differences ($n=3$, $p<0.05$) u.l. undetectable level

the increase of pyrolysis without significant difference at the two higher temperatures ($p<0.05$), whereas Na^{+} and K^{+} first increased and then decreased with increasing pyrolysis temperature with no significant difference at the higher temperatures. Compared to other studies, these results suggest considerable variation of pyrolysis temperature influence on these cations. For example, Rafiq et al. (2016) reported increase in all four cations for corn stover biochars as pyrolysis temperature increases. On the other hand, Chen et al. (2014) reported increase of Ca^{2+} and Mg^{2+} and irregular trends of K^{+} and Na^{+} in relation to pyrolysis temperatures.

In addition to the parameters in Table 1 influencing the sorption mechanisms, they also influence each other. The CEC of MBC showed significantly positive correlation with K^{+}, Na^{+} and pH ($r=1.00$, $r=0.99$ and $r=0.81$, respectively; $p<0.01$) and non-significant negative correlation with Mg^{2+} ($r=-0.67$) and non-significant positive correlation with Ca^{2+} ($r=0.47$) (Table 2).

These parameters can also play crucial role indirectly through their influences on each other. For instance, the high concentrations of Na^{+} and K^{+} in the studied biochars are the main reasons behind high pH (with a significantly positive correlation of $r=0.85$ and $r=0.82$; respectively; $p<0.01$). Various studies (Chen et al. 2014; Jin et al. 2016; Wang et al. 2015a) explained the reasons for pH increases with pyrolysis temperature. The first study attributed the increase of pH as pyrolysis temperature increase to the release of alkali salts from pyrolytic structure whereas the latter studies indicated the cause to be the ash contents.

The high pH of biochar prompts the CEC and in turn increase electrostatic interaction which reduce bioavailability of metals (Forján et al. 2018; Tomczyk et al. 2019). Each biochar also reduced the available Cu^{2+} to below detection level and greatly for Zn^{2+}. This in agreement with that have been demonstrated by other studies (Forján et al. 2018; Karami et al. 2011).

Regarding the biochars produced from two different biomasses at the same temperature and condition, the parameters were significantly different from each other except for EC extractable Zn^{2+} (Table 3). The role of biomass in sorption capacity of the biochars is discussed in the following section by comparing the two biochars pyrolyzed at the same temperature.

Sorption isotherms

The accuracy of sorption processes is determined by successful modeling and interpretation of sorption isotherms. There are numerous sorption isotherm models and they function based on various assumptions. The selection and configuration of models are determined by estimation of model parameters. The accuracy of a given model is determined by statistical error measures. The coefficient of determinations (R^2) is one of common error measures (Ayawei et al., 2017; Bharat, 2017). Both Langmuir and

Table 2 Pearson correlation

	N %	C %	C/N	pH	EC mS/cm	Ca	K	Mg	Na	Temp	Zn2	CEC	Cu 1
N %													
C %	−0.20												
C/N	−0.96**	0.43											
pH	−0.72*	0.75*	0.84**										
EC mS/cm	−0.38	0.92**	0.51	0.87**									
Ca	0.50	−0.85**	−0.67*	−0.87**	−0.83**								
K	−0.90**	0.30	0.89**	0.82**	0.50	−0.55							
Mg	0.63	−0.74*	−0.75*	−0.90**	−0.74*	0.97**	−0.68*						
Na	−0.89**	0.37	0.91**	0.85**	0.58	−0.58	0.99**	−0.69*					
Zn2	−0.59	0.85**	0.74*	0.95**	0.87**	−0.87**	0.66	−0.88**	0.70*	0.93**			
CEC	−0.89**	0.27	0.88**	0.81**	0.50	−0.54	1.00**	−0.67	0.99**	0.47	0.65		
Cu 1	−0.25	0.91**	0.48	0.82**	0.90**	−0.88**	0.44	−0.80*	0.49	0.93**	0.86**	0.43	
Zn 1	−0.77*	0.47	0.82**	0.79*	0.60	−0.82**	0.71*	−0.85**	0.71*	0.61	0.65	0.70*	0.56

**Correlation is significant at the 0.01 level (2-tailed)

*Correlation is significant at the 0.05 level (2-tailed)

Table 3 Physicochemical characterization of biochars based on feedstock biomass

Parameters	Biochar			P
		MB500	QB500	
pH		10.26 ± 0.04a	8.84 ± 0.02b	***
EC	mS/cm	2.23 ± 0.23a	2.11 ± 0.23a	n.s
C	%	64.55 ± 0.37b	70.99 ± 0.23a	***
N		0.34 ± 0.04b	0.65 ± 0.04a	**
C/N		193.81 ± 25.20a	108.90 ± 6.17b	**
Pseudo total				
Cu^{2+}	(mg kg^{-1})	10.44 ± 0.39b	18.72 ± 0.47a	***
Pb^{2+}		u.l	u.l	
Zn^{2+}		131.10 ± 27.48a	66.53 ± 11.68b	*
Extractable				
Cu^{2+}	(mg kg^{-1})	u.l	u.l	
Pb^{2+}		u.l	u.l	
Zn^{2+}		1.28 ± 0.17a	0.24 ± 0.11a	**
CEC	(cmol $_{(\pm)}$ kg^{-1})	50.54 ± 4.73a	24.57 ± 3.27b	**
Ca^{2+}		0.17 ± 0.02b	10.99 ± 1.58a	***
K^{+}		49.50 ± 4.65a	5.13 ± 0.53b	***
Mg^{2+}		0.29 ± 0.02b	8.14 ± 1.14a	***
Na^{+}		0.58 ± 0.05a	0.31 ± 0.04b	**

For each row, different letters in different samples mean significant differences ($n = 3$, $p < 0.05$, $p < 0.01$, $p < 0.001$ for *, **, ***, respectively), n.s. nonsignificant, u.l. undetectable level

Freundlich models are popularly used models in batch sorption experiments (Forján et al. 2016; Rodríguez-Vila et al. 2018).

The goodness of fit (R^2) values were used to select most suitable model for isotherm parameters. The corresponding values are presented below both for Langmuir and Freundlich models in Table 4. However, not all isotherms fitted the Langmuir or Freundlich model. As shown in Table 4, the sorption isotherms of Cu^{2+} fitted the Langmuir model, except for MB500. Regarding Freundlich model, the sorption isotherms of Cu^{2+} fitted only for QB500 and MB350.

The sorption isotherm of Pb^{2+} fitted the Langmuir model except for MB650. The sorption isotherm of Pb^{2+} did not fit the Freundlich model except for QB500. The sorption isotherms of Zn^{2+} fitted the Langmuir model for all biochars. The sorption isotherms for Zn^{2+} did not fit the Freundlich model, except for QB500. Since the isotherms did not fit neither the Langmuir model nor the Freundlich for some biochars, it is impossible to use the models' outputs to compare sorption capacity of biochars. Therefore, sorption distribution coefficients (K_d) were calculated to estimate the sorption capacity of studied biochars. The K_d is also an important parameter in describing the mobility of metals in the soil (Park et al. 2016; Yaacob et al. 2008).

Estimation of the sorption capacity using the distribution coefficient K_d and %MR

The sorption curves were irregular except for QB500. This is because metals such as Cu^{2+}, Pb^{2+}, and Zn^{2+} are known to usually coexist (Chen et al. 2011; Uchimiya et al. 2010) and they compete for sorption sites leading to irregular sorption isotherms (Cerqueira et al. 2011; Park et al. 2016; Vega et al. 2006). The sorption coefficient of distribution (K_d) and of percentage of metal removal (%MR) given in Table 5 show the sorption capacities of biochars used in this study.

Metals sorption can be distributed among different mechanisms such as metal exchange with cations, complexation

Table 4 Langmuir and Freundlich isotherms parameters

Langmuir					Freundlich		
Metal	Biochar	R^2	β_L ($\mu molg^{-1}$)	K_L ($\times 10^3$ $L\mu mol^{-1}$)	R^2	n	K_F ($L\ g^{-1}$)
Cu^{2+}	QB500	0.89	69.44	250.43	0.90	1.428	12.703
	MB350	0.98	29.851	14.00	0.40	1.904	2.072
	MB500	0.03	149.25	2.24	0.31	1.677	2.010
	MB650	0.72	69.44	5.11	0.76	2.653	2.288
Pb^{2+}	QB500	0.99	42.372	11,800	0.81	3.11	33.23
	MB350	0.99	22.67	64.06	0.33	6.09	14.79
	MB500	0.82	10.62	−421.21	0.09	−6.41	35.60
	MB650	0.18	29.58	41.49	0.57	3.94	3.84
Zn^{2+}	QB500	0.99	41.15	55.75	0.83	2.34	3.62
	MB350	0.94	1.22	−6.33	0.35	5.78	4.66
	MB500	0.97	16.66	−16.52	0.56	3.85	4.04
	MB650	0.95	10.22	−13.23	0.06	−11.66	5.14

Table 5 Kd values and metal removal percentage

Metal	Biochar	%MR	K_d ($L\ kg^{-1}$)
Cu^{2+}	QB500	99.82	13,961.10a
	MB350	81.37	343.54b
	MB500	91.88	982.30b
	MB650	90.58	624.41b
Pb^{2+}	QB500	99.96	93,491.19a
	MB350	83.11	1019.93b
	MB500	95.54	3606.09b
	MB650	96.72	3247.64b
Zn^{2+}	QB500	94.71	3679.35a
	MB350	51.85	200.71c
	MB500	73.40	563.19b
	MB650	70.35	619.49b

Different letters indicate significant differences within the same column corresponding to metals at p value < 0.05

with functional groups and surface precipitation (Zhou et al. 2019). In-depth analysis of sorption mechanisms is beyond the scope of this study. However, literature shows how these mechanisms differ depending on the metals and types of biochar (Li et al. 2017; Lu et al. 2012). According to Lu et al. (2012), cation exchange with Ca^{2+} and Mg^{2+} accounted for 40–52% of whereas K^+ and Na^+ contributed for 4.8–8.5% for Pb^{2+} sorption by biochar produced from sludge. The same study reported 38–42% of lead was removed by complexation with carboxyl and hydroxyl groups. Ding et al. (2014) also attributed 62% of Pb^{2+} sorption by bagasse biochar to cations exchange. Li et al. (2017) explained the role of these cations, i.e., Ca^{2+} Mg^{2+} Na^+ and K^+ and other minerals such as phosphorous as they can either exchange or precipitate to reduce the metal availability. At pH > 7 Cu^{2+}, Pb^{2+} and Zn^{2+} were dominantly removed by chemical precipitation as their solubility decreases (Malamis et al. 2011).

Rodríguez-Vila et al. (2018) reported Cu^{2+} and Zn^{2+} sorption exponentially increased as C/N ratio decreased. However, our result is contrary to their findings. This is probably due to difference in feedstock biomass used to produce biochar. The sorption distribution coefficients of studied biochars corresponded with C/N ratio except for Zn^{2+} as shown in Tables 1 and 5. The correlation coefficients of C/N and K_d which were 0.97, 0.98, and 0.90 for Cu^{2+}, Pb^{2+}, and Zn^{2+}, respectively, further demonstrated this correspondence. However, the C/N ratio did not have any statistically significant impact ($p < 0.05$), as the order of sorption capacity was the contrary to the suggestion above. The other phenomena we observed was the influence of the concentrations of added metals. The competitions for sorption sites were more pronounced between Cu^{2+} and Zn^{2+}. However, it is interesting to note their competition was significantly small at the lower concentration compared to swift competition at higher concentrations (> 1 mM, Fig. 1). This is most probably because at lower concentration they were sorbed onto different abundantly available sites (Chen et al. 2011; Wang et al. 2015b**).** Song et al. (2019) demonstrated the influence of ionic strength on metal sorption by biochar where the influence on copper was greater than influence on chromium. The variations among the biochars used in this study are explained below.

Metal removal capacities of maize biochars in each concentration for each metal were also evaluated. At lower concentrations (0.1–1 mM), Pb^{2+} and Cu^{2+} were sorbed the most by MB350 followed by MB650. However, at the two higher concentrations (2 and 3 mM) the trend switched to MB500 > MB650 > MB350 (Fig. 1). Statistically, Cu^{2+} removal by MB350 at 1 mM was significantly different for all concentrations whereas the two lower concentrations

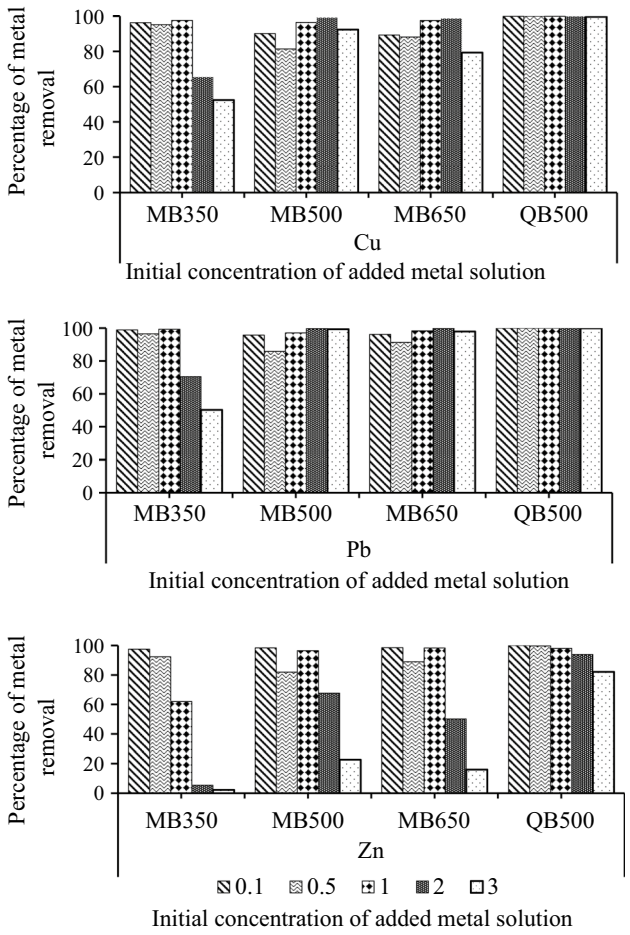

Fig. 1 Percentage of metal removal from each concentration

(0.1 and 0.5 mM) did not have significant difference at $p < 0.05$. Similarly, the two higher concentrations were not significantly different from each other but different from the rest at $p < 0.05$. The same trends were observed for Pb^{2+} except 0.5 mM which was not statistically different from any concentration at $p < 0.05$. The studied biochars wise, Pb^{2+} and Cu^{2+} removals by MB350 was different from MB500 and MB650 except at 1 mM for both and 0.5 mM for MB650 at $p < 0.05$. The other two maize biochars (MB500 and MB650) were not significantly different from each other except for Cu^{2+} at 3 mM at $p < 0.05$. The individual %MR for each concentration shows the difference in sorption behavior at the lower and higher concentrations (Fig. 1). This is important to select the ideal biochar metal sorption. In this study, MB650 had higher %MR at lower concentrations, but MB500 was more effective in terms of overall sorption capacity and had higher %MR at higher concentrations (Fig. 1).

The removal of Zn^{2+} followed MB650 > MB500 > MB350 sequence order at lower concentrations except the sequence at 0.5 mM was MB350 > MB650 > MB500. They were not significantly different from each other except 0.5 mM for MB500 at $p < 0.05$. At the two higher concentrations (2 and 3 mM), MB500 removed more Zn^{2+} than the other two maize cob biochars. Statistically, MB350 was significantly different from both except from MB650 at 0.5 mM, whereas MB500 and MB650 were significantly different only at 2 mM at $p < 0.05$. The MB350 was not only the least, but %MR dropped from 97.43% at 0.1 mM to 2.23% at 3 mM for Zn^{2+} (Fig. 1). Similarly, %MR by MB350 at two higher concentrations decreased from 98.95% to 50.3% and 96.28% to 52.4% for Pb^{2+} and Cu^{2+} at 0.1 mM and 3 mM, respectively. Zn^{2+} removal also decreased significantly in the MB650 and MB500 at the higher concentrations compared to the other two metals. Generally, competitions for sorption sites were stronger in maize cob biochars than in *Quercus ilex* L. biochar. The competition was more intense at higher concentrations for Zn^{2+} and MB350 for all the three metals Fig. 1. However, there were certain cases where less metals were removed at lower concentrations in MB500 and MB650. These are due to the same reason explained above for isotherm curves irregularity.

Despite being most effective sorbent as shown by K_d and %MR in Table 5, the QB500 biochar did not have the highest value for each parameter shown in Table 3. This indicates the role of feedstock biomass in sorption capacity of biochar when pyrolyzed at the same temperature.

Biomass with a high C/N ratio often suggests the presence of high amount of lignin and cellulose. This affects sorption capacity negatively when combined with low level of nitrogen (Rodríguez-Vila et al. 2018). These author's general suggestion is that Cu^{2+} and Zn^{2+} sorptions are enhanced as C/N decreases. Although MB350 comparatively had the lowest C/N ratio, it was the least favorable biochar for sorption of all studied metals. This could be due to different biomass they used and the lowest pyrolysis temperature which plays critical role which was far below the suggested optimal pyrolysis temperature for cob biochar is 588.42 °C (Intani et al. 2018). Regarding the role of feedstock material QB500 had the least C/N among four types of biochar, yet it had highest %MR and K_d.

The other important factor that favors sorption of Cu^{2+} over Zn^{2+} is the higher electronegativity of Cu^{2+} and its greater charge to radius ratio (McBride, 1994) and this results in a greater bond of Cu^{2+} with functional groups of the biochar (Rodríguez-Vila et al. 2018). Our results agree with this explanation based on the overall sequence of studied metals sorption which correspond to their degree of electronegativity.

Chen et al. (2011) explained the effect of pyrolysis temperature to be greater than the biomass feedstock on sorption curves and structural characteristics. On the other hand, Sun et al. (2014) highlighted the difference in sorption capacity of biochars pyrolyzed under the same condition but different biomass. In our study, two biochars pyrolyzed at the same

temperature (500 °C) which were sourced from *Quercus ilex* L. and *Zea mays* L. cob exhibited clearly different characteristics (Table 3). For biochars pyrolyzed under the same condition, the biochar original raw material composition played a major role in determining the biochars sorption capacities. Consequently, QB500 had a higher %MR and K_d compared to MB500 pyrolyzed under the same condition and temperature. Therefore, we attribute their difference to biomass feedstock. It is also important to take into consideration the optimal pyrolysis temperature for a given biomass feedstock. When a given biomass is pyrolyzed at the right temperature, it will result in biochar with a higher sorption capacity. This was confirmed based on the sorption capacities of MB500 and MB650.

Selective sequences of studied metals

The overall selective sequences of each metal for every biochar in this study are established using sorption distribution coefficient (K_d). The sequences follow $Pb^{2+} > Cu^{2+} > Zn^{2+}$ in all biochars. Consequently, Pb^{2+} was more favorably sorbed than the other two metals by all biochars ($p < 0.05$). It is interesting to note Pb^{2+} is the most competitive among the three metals (Table 5). This has been the case even when different amendments were used (Covelo et al. 2007; Forján et al. 2016; Maradona et al. 2020). These studies attributed the phenomena to the high organic matter content as a reason of why Pb^{2+} was the most competitive.

Our results indicate the competition for sorption sites affected the sorption of Zn^{2+} more than Pb^{2+} and Cu^{2+}. This shows Zn^{2+} can be easily exchanged and replaced by either of the two metals. Park et al. (2016) reported the same regarding the selective sequence of Pb^{2+} and Cu^{2+} against Cd^{2+} and Zn^{2+}. Furthermore, Zn^{2+} had little effect on sorption of Cu^{2+} even at a higher concentration (Chen et al. 2011). The lower K_d values of Zn^{2+} indicate that it was easily exchanged with and replaced by Pb^{2+} and Cu^{2+}. This result agrees with the findings by Covelo et al. (2007), Deng et al. (2017) and Park et al. (2016).

Conclusion

The results of this study indicate the sorption behavior of metals varies based on feedstock biomass, pyrolysis temperatures and the corresponding concentration of sorption solutions. These underlying mechanisms are important serving as a guideline starting from biochar production under desirable conditions to their application for removal of targeted metals.

Accordingly, the K_d values of QB500 are 13,961.1, 93,491.19, and 3679.35 Lkg^{-1} compared to 982.3, 3606.09, 563.19 Lkg^{-1} of MB500 for Cu^{2+}, Pb^{2+} and Zn^{2+}, respectively. This indicates the role of biomass for biochars pyrolyzed under the same conditions. The impact of pyrolysis temperature on biochar characteristics and sorption capacity is conspicuous. However, it is important to pyrolysis them at the optimum temperature to obtain desirable quality. Among maize cobs biochars, biochar pyrolyzed at MB500 was more effective than MB350 and MB650 having higher K_d values except for MB650 for Zn^{2+} which is 619.49 Lkg^{-1} compared to 563.19 Lkg^{-1} for MB500. This indicates the importance of biomass pyrolysis at the right temperature, which is below 600 °C to produce ideal maize cob biochar.

Finally, it is important to consider the metal removal percentage differences in combination of pyrolysis temperature and metal concentrations. The metal removal percentage differences among biochars at lower concentrations of added metal solutions were very low compared to higher concentrations where competitions for sorption sites are greater.

Acknowledgements The authors wish to thank all who assisted in conducting this work.

Authors contributions Mati Amano Geleto: Designed and carried out the experiment. Wrote the manuscript with support from co-authors contribution to the interpretation of the results. Rubén Forján Castro: Contributed to sample preparation and contributed to the interpretation of the results. Provided critical review in data analysis and writing the manuscript. Elena Arco-Lázaro: Performed the analytic calculations and data analysis. Provided critical review in data analysis and writing the manuscript. Emma Fernandez Covelo: Supervised the experiment by verifying the analytical methods. Contributed to the data analysis and interpretation of the results. Provided critical review in manuscript writing. Purificación Marcet Miramontes: Contributed to conceptualization of the study and critical review in drafting and revision. Beatriz Cancelo Cerqueira: Contributed to sample preparation and contributed to the interpretation of the results. Provided critical review in data analysis and writing the manuscript. All authors provided discussion of the results and contributed to the manuscript by providing critical feedback, shaping the research, data analysis and discussing results.

Funding Open Access funding provided thanks to the CRUE-CSIC agreement with Springer Nature. No funding was provided for this study.

Data availability Data will be made available upon request.

Declarations

Conflict of interest The authors declare that they have no conflicts of interest.

Human and animal rights This study did not involve any human participants and/or animals.

Open Access This article is licensed under a Creative Commons Attribution 4.0 International License, which permits use, sharing, adaptation, distribution and reproduction in any medium or format, as long as you give appropriate credit to the original author(s) and the source, provide a link to the Creative Commons licence, and indicate if changes were made. The images or other third party material in this article are included in the article's Creative Commons licence, unless indicated otherwise

in a credit line to the material. If material is not included in the article's Creative Commons licence and your intended use is not permitted by statutory regulation or exceeds the permitted use, you will need to obtain permission directly from the copyright holder. To view a copy of this licence, visit http://creativecommons.org/licenses/by/4.0/.

References

Ahmad M, Lee SS, Dou X, Mohan D, Sung JK, Yang JE, Ok YS (2012) Effects of pyrolysis temperature on soybean stover- and peanut shell-derived biochar properties and TCE adsorption in water. Biores Technol 118:536–544

Ahmad M, Ok YS, Rajapaksha AU, Lim JE, Kim BY, Ahn JH, Lee YH, Al-Wabel MI, Lee SE, Lee SS (2016) Lead and copper immobilization in a shooting range soil using soybean stover– and pine needle–derived biochars: chemical, microbial and spectroscopic assessments. J Hazardous Mater 301:179–186

Ahmad M, Rajapaksha AU, Lim JE, Zhang M, Bolan N, Mohan D, Ok YS (2014) Biochar as a sorbent for contaminant management in soil and water: a review. Chemosphere 99:19–33

Alberti G, Cristini A, Loi A, Melis P, Pilo G (1997) Copper and lead sorption by different fractions of two Sardinian soils. In: Prost R (ed) Contaminated Soils: Third International Conference on the Biogeochemistry of trace-elements [CD-ROM]. INRA editions, Paris

Ayangbenro A, Babalola O (2017) A New strategy for heavy metal polluted environments: a review of microbial biosorbents. Int J Environ Res Public Health 14:94

Ayawei N, Ebelegi AN, Wankasi D (2017) Modelling and interpretation of adsorption isotherms. J Chem 2017:1–11

Barakat MA (2011) New trends in removing heavy metals from industrial wastewater. Arab J Chem 4:361–377

Beesley L, Marmiroli M (2011) The immobilisation and retention of soluble arsenic, cadmium and zinc by biochar. Environ Pollut 159:474–480

Bharat TV (2017) Selection and configuration of sorption isotherm models in soils using artificial bees guided by the particle swarm. Adv Artif Intell 2017:1–22

Cerqueira B, Covelo EF, Andrade LM, Vega FA (2011) The influence of soil properties on the individual and competitive sorption and desorption of Cu and Cd. Geoderma 162:20–26

Cetin B (2016) Investigation of PAHs, PCBs and PCNs in soils around a heavily industrialized area in Kocaeli, Turkey: concentrations, distributions, sources and toxicological effects. Sci Total Environ 560–561:160–169

Chen T, Zhang Y, Wang H, Lu W, Zhou Z, Zhang Y, Ren L (2014) Influence of pyrolysis temperature on characteristics and heavy metal adsorptive performance of biochar derived from municipal sewage sludge. Biores Technol 164:47–54

Chen X, Chen G, Chen L, Chen Y, Lehmann J, McBride MB, Hay AG (2011) Adsorption of copper and zinc by biochars produced from pyrolysis of hardwood and corn straw in aqueous solution. Biores Technol 102:8877–8884

Covelo EF, Vega FA, Andrade ML (2007) Heavy metal sorption and desorption capacity of soils containing endogenous contaminants. J Hazard Mater 143:419–430

Deng J, Liu Y, Liu S, Zeng G, Tan X, Huang B, Yan Z (2017) Competitive adsorption of Pb(II), Cd(II) and Cu(II) onto chitosan–pyromellitic dianhydride modified biochar. J Colloid Interface Sci 506:355–364

Desta MB (2013) Batch sorption experiments: Langmuir and Freundlich isotherm studies for the adsorption of textile metal ions onto teff straw (*Eragrostis tef*) agricultural waste. Journal of Thermodynamics 2013:1–6

Ding W, Dong X, Ime IM, Gao B, Ma LQ (2014) Pyrolytic temperatures impact lead sorption mechanisms by bagasse biochars. Chemosphere 105:68–74

Dong X, Ma LQ, Li Y (2011) Characteristics and mechanisms of hexavalent chromium removal by biochar from sugar beet tailing. J Hazard Mater 190:909–915

Elzobair KA, Stromberger ME, Ippolito JA, Lentz RD (2016) Contrasting effects of biochar versus manure on soil microbial communities and enzyme activities in an Aridisol. Chemosphere 142:145–152

Forján R, Asensio V, Rodríguez-Vila A, Covelo EF (2016) Contribution of waste and biochar amendment to the sorption of metals in a copper mine tailing. CATENA 137:120–125

Forján R, Rodríguez-Vila A, Covelo EF (2018) Using compost and technosol combined with biochar and *Brassica juncea* L. to decrease the bioavailable metal concentration in soil from a copper mine settling pond. Environ Sci Pollut Res 25:1294–1305

Gomes PC, Fontes MPF, da Silva AG, de S. Mendonça E, Netto AR, (2001) Selectivity sequence and competitive adsorption of heavy metals by Brazilian soils. Soil Sci Soc Am J 65:1115–1121

Harter RD, Naidu R (2001) An assessment of environmental and solution parameter impact on trace-metal sorption by soils. Soil Sci Soc Am J 65:597–612

Hendershot WH, Duquette M (1986) A simple barium chloride method for determining cation exchange capacity and exchangeable cations. Soil Sci Soc Am J 50:605–608

Hotová G, Slovák V (2015) Effect of pyrolysis temperature and thermal oxidation on the adsorption properties of carbon cryogels. Thermochim Acta 614:45–51

Intani K, Latif S, Cao Z, Müller J (2018) Characterisation of biochar from maize residues produced in a self–purging pyrolysis reactor. Biores Technol 265:224–235

Inyang MI, Gao B, Yao Y, Xue Y, Zimmerman A, Mosa A, Pullammanapallil P, Ok YS, Cao X (2016) A review of biochar as a low–cost adsorbent for aqueous heavy metal removal. Crit Rev Environ Sci Technol 46:406–433

Jin J, Li Y, Zhang J, Wu S, Cao Y, Liang P, Christie P (2016) Influence of pyrolysis temperature on properties and environmental safety of heavy metals in biochars derived from municipal sewage sludge. J Hazard Mater 320:417–426

Kaplan DI, Seme RJ, Piepkho MG (1995) Geochemical factors affecting radionuclide transport through near and far fields at a Low-Level Waste Disposal Site available sorption constants and recommendations for future studies. Pacific Northwest National Laboratory, Richland

Karami N, Clemente R, Moreno-Jiménez E, Lepp NW, Beesley L (2011) Efficiency of green waste compost and biochar soil amendments for reducing lead and copper mobility and uptake to ryegrass. J Hazard Mater 191:41–48

Klasson KT (2017) Biochar characterization and a method for estimating biochar quality from proximate analysis results. Biomass Bioenerg 96:50–58

Kloss S, Zehetner F, Dellantonio A, Hamid R, Ottner F, Liedtke V, Schwanninger M, Gerzabek MH, Soja G (2012) Characterization of slow pyrolysis biochars: effects of feedstocks and pyrolysis temperature on biochar properties. J Environ Quality 41:990–1000

Kumar R, Rani M, Gupta H, Gupta B (2014) Trace metal fractionation in water and sediments of an urban river stretch. Chem Speciat Bioavailab 26:200–209

Kupryianchyk D, Hale S, Zimmerman AR, Harvey O, Rutherford D, Abiven S, Knicker H, Schmidt HP, Rumpel C, Cornelissen G (2016) Sorption of hydrophobic organic compounds to a diverse suite of carbonaceous materials with emphasis on biochar. Chemosphere 144:879–887

Li H, Dong X, da Silva EB, de Oliveira LM, Chen Y, Ma LQ (2017) Mechanisms of metal sorption by biochars: Biochar characteristics and modifications. Chemosphere 178:466–478

Li J, Xu Y (2015) Immobilization of Cd in paddy soil using moisture management and amendment. Environ Sci Pollut Res 22(7):5580–5586

Liu X, Zhang Y, Li Z, Feng R, Zhang Y (2014) Characterization of corncob–derived biochar and pyrolysis kinetics in comparison with corn stalk and sawdust. Biores Technol 170:76–82

Lu H, Zhang W, Yang Y, Huang X, Wang S, Qiu R (2012) Relative distribution of Pb2+ sorption mechanisms by sludge–derived biochar. Water Res 46:854–862

Malamis S, Katsou E, Haralambous KJ (2011) Study of Ni(II), Cu(II), Pb(II), and Zn(II) removal using sludge and minerals followed by MF/UF. Water Air Soil Pollut 218:81–92

Maradona I, Kanus JH, Stephen MS (2020) Sorption of Pb^{2+}, Cu^{2+} and Zn^{2+} from aqueous solution using a blended membrane of immobilized karkashi (sesame leaves) and sodium alginate. Chem Sci Int J 29:21–29

McBride MB (1994) Environmental chemistry of soils. Oxford Univ. Press, New York

Melo LCA, Coscione AR, Abreu CA, Puga AP, Camargo OA (2013) Influence of pyrolysis temperature on cadmium and zinc sorption capacity of sugar cane straw-derived biochar. BioResources 8:4992–5004

Novak JM, Lima I, Xing B, Gaskin JW, Steiner C, Das KC, Ahmedna M, Rehrah D, Watts DW, Busscher WJ, Schomberg H (2009) Characterization of designer biochar produced at different temperatures and their effects on a loamy sand. Ann Environ Sci 3:195–206

Park J-H, Ok YS, Kim S-H, Cho J-S, Heo J-S, Delaune RD, Seo D-C (2016) Competitive adsorption of heavy metals onto sesame straw biochar in aqueous solutions. Chemosphere 142:77–83

Puga AP, Abreu CA, Melo LCA, Beesley L (2015) Biochar application to a contaminated soil reduces the availability and plant uptake of zinc, lead and cadmium. J Environ Manag 159:86–93

Qian K, Kumar A, Zhang H, Bellmer D, Huhnke R (2015) Recent advances in utilization of biochar. Renew Sustain Energy Rev 42:1055–1064

Qu C, Albanese S, Chen W, Lima A, Doherty AL, Piccolo A, Arienzo M, Qi S, De Vivo B (2016) The status of organochlorine pesticide contamination in the soils of the Campanian Plain, southern Italy, and correlations with soil properties and cancer risk. Environ Pollut 216:500–511

Rafiq MK, Bachmann RT, Rafiq MT, Shang Z, Joseph S, Long R (2016) Influence of pyrolysis temperature on physico-chemical properties of corn stover (*Zea mays* L.) biochar and feasibility for carbon capture and energy balance. PLoS ONE 11(6):e0156894

Rodríguez-Vila A, Selwyn-Smith H, Enunwa L, Smail I, Covelo EF, Sizmur T (2018) Predicting Cu and Zn sorption capacity of biochar from feedstock C/N ratio and pyrolysis temperature. Environ Sci Pollut Res 25:7730–7739

Rosales E, Ferreira L, Sanromán MÁ, Tavares T, Pazos M (2015) Enhanced selective metal adsorption on optimised agroforestry waste mixtures. Biores Technol 182:41–49

Sanchez-Monedero MA, Cayuela ML, Roig A, Jindo K, Mondini C, Bolan N (2018) Role of biochar as an additive in organic waste composting. Biores Technol 247:1155–1164

Song J, He Q, Hu X, Zhang W, Wang C, Chen R, Wang H, Mosa A (2019) Highly efficient removal of Cr (VI) and Cu (II) by biochar derived from *Artemisia argyi* stem. Environ Sci Pollut Res 26:13221–13234

Sohi S, Lopez-Capel E, Krull E, Bol R (2009) Biochar, climate change and soil: a review to guide future research. CSIRO Land Water Sci Rep 5:17–31

Steiner C (2016) Considerations in biochar characterization. In: Guo M, He Z, Uchimiya SM (eds) Agricultural and environmental applications of biochar: advances and barriers. SSSA, Madison, pp 87–100

Sun J, Lian F, Liu Z, Zhu L, Song Z (2014) Biochars derived from various crop straws: characterization and Cd(II) removal potential. Ecotoxicol Environ Saf 106:226–231

Swartjes FA (2011) Introduction to contaminated site management. In: Swartjes FA (ed) Dealing with contaminated sites. Springer, Dordrecht, pp 3–89

Tan X, Liu Y, Zeng G, Wang X, Hu X, Gu Y, Yang Z (2015) Application of biochar for the removal of pollutants from aqueous solutions. Chemosphere 125:70–85

Tomczyk A, Boguta P, Sokołowska Z (2019) Biochar efficiency in copper removal from Haplic soils. Int J Environ Sci Technol 16:4899–4912

Tóth G, Hermann T, Da Silva MR, Montanarella L (2016) Heavy metals in agricultural soils of the European Union with implications for food safety. Environ Int 88:299–309

Uchimiya M, Bannon DI, Wartelle LH, Lima IM, Klasson KT (2012) Lead retention by broiler litter biochars in small arms range soil: impact of pyrolysis temperature. J Agric Food Chem 60:5035–5044

Uchimiya M, Lima IM, Klasson TK, Chang S, Wartelle LH, Rodgers JE (2010) Immobilization of heavy metal ions (CuII, CdII, NiII, and PbII) by Broiler Litter–Derived Biochars in water and soil. J Agric Food Chem 58:5538–5544

Vega FA, Covelo EF, Andrade ML (2006) Competitive sorption and desorption of heavy metals in mine soils: Influence of mine soil characteristics. J Colloid Interface Sci 298:582–592

Vega FA, Covelo EF, Andrade ML (2008) A versatile parameter for comparing the capacities of soils for sorption and retention of heavy metals dumped individually or together: results for cadmium, copper and lead in twenty soil horizons. J Colloid Interface Sci 327:275–286

Wang H, Gao B, Wang S, Fang J, Xue Y, Yang K (2015a) Removal of Pb (II), Cu (II), and Cd (II) from aqueous solutions by biochar derived from KMnO4 treated hickory wood. Biores Technol 197:356–362

Wang X, Zhou W, Liang G, Song D, Zhang X (2015b) Characteristics of maize biochar with different pyrolysis temperatures and its effects on organic carbon, nitrogen and enzymatic activities after addition to fluvo-aquic soil. Sci Total Environ 538:137–144

Yaacob WZW, Samsudin AR, Kong TB (2008) The sorption distribution coefficient of lead and copper on the selected soil samples from Selangor. Bull Geol Soc Malaysia 54:21–25

Zhao M, Dai Y, Zhang M, Feng C, Qin B, Zhang W, Zhao N, Li Y, Ni Z, Xu Z, Tsang DCW, Qiu R (2020) Mechanisms of Pb and/or Zn adsorption by different biochars: Biochar characteristics, stability, and binding energies. Sci Total Environ 717:136894

Zhou H, Meng H, Zhao L, Shen Y, Hou Y, Cheng H, Song L (2018) Effect of biochar and humic acid on the copper, lead, and cadmium passivation during composting. Biores Technol 258:279–286

Zhou N, Zu J, Feng Q, Chen H, Li J, Zhong ME, Zhou Z, Zhuang S (2019) Effect of pyrolysis condition on the adsorption mechanism of heavy metals on tobacco stem biochar in competitive mode. Environ Sci Pollut Res 26:26947–26962